Role of Active Tectonism and Geomorphic Drivers on Channel Oscillation of the Raidak-I River in the Eastern Himalayan Foothills, India

Md. Hasanuzzaman, Pravat Kumar Shit, and Aznarul Islam

Abstract The dynamicity of the channel is the main characteristic of the Raidak-I River in the eastern Himalayan foothill. The present study evaluates riverbank migration in association with erosion–deposition changes along the river Raidak-I using DSAS models. The present work intends to evaluate the relationship between the riverbank erosion–deposition and geomorphological and tectonic adjustment. For the study, earth observatory data like MSS, TM, ETM+ and OLI datasets of 1972, 1979, 1987, 1995, 2003, 2011, and 2020 have been used to demarcate the bankline position. Temporal analysis reveals that the river has changed its bank position by extensive erosion-accretion processes and modified its floodplain area uses significantly. The historical positions of both banklines indicate that a large portion of the floodplain area depicts an erosion-accretion sequence with time. In the timeframe of the last 48 years, the Raidak-I River has an average erosion–deposition at −0.23 m/year on the right bank and 1.57 m/y on the left bank. A general observation from this research is that the most dynamic or migrant part of the river is zone A and zone B compared to zone C which is relatively stable. In this study, the river course in zone C (both banks) is the most dynamic part of this entire river. The changes by the direct effect of banking migration have a bad impact on the dwellers of the floodplain adjacent village area of the river. The results of this study can represent an important indicator of the vulnerability of the Raidak-I River buffer area and also provide information about the geomorphological instabilities of the study area.

Keywords DSAS · Erosion–deposition · Himalayan foothill · Alluvial channel · Remote sensing

Md. Hasanuzzaman · P. K. Shit (✉)
PG Department of Geography Raja N. L, Khan Women's College (Autonomous), Midnapore 721102, India

A. Islam
Department of Geography, Aliah University, 17 Gora Chand Road, Kolkata 700014, India

1   Introduction

The foothills region of an active orogenic belt such as the Himalayas is characterized by active faults and complex alluvial morphology with fluvial erosion and deposition (Burbank and Anderson 2001). The eastern Himalayan foothills, east of the Tista River in West Bengal depicted a large piedmont area, which is drained by numerous major and minor rivers. These rivers brought immense load from the Himalayas in form of boulders, gravels, sand, and silt, and deposit the coarser ones at the foothills in the extreme north due to lesser slopes (Starkel et al. 2008) while accrete the finer particles in the south (parts of Darjeeling, Jalpaiguri and Alipurduar districts and entire Coochbehar district) to form and shape their wide, flat and almost monotonous floodplains subjected to inundation for multiple times even in a single monsoon season hampering the livelihoods of the floodplain dwellers. An alluvial river floodplain area of the Himalayan foothills experiences frequent periodical and seasonal variations as a result of channel migration through erosion deposition (Bastawesy et al. 2013). The channel migration, high sediment load, frequent floods, and anthropogenic interventions have caused morphological changes in the river course (Kuehl et al. 2005; Kummu et al. 2008; Guchhait et al. 2016). Meandering rivers signify channel dynamicity which reveals frequent changes in channel patterns through bank erosion, deposition, down cutting, etc. (Uddin et al. 2011). River meander and channel shifting are very complex processes of river floodplains that are triggered by different factors in the fluvial system (Hooke 2013; Islam and Guchhait 2017a). Channel migration is one of the significant characteristics that can change the morphology of river buffer areas, with major problems for human life (Gurnell et al. 2012; Islam and Guchhait 2017b). River geomorphological factors are important indicators to investigate environmental changes and are especially related to changes in river buffer areas (Dai et al. 2008). These geomorphological changes are associated with changes in sediment load and river discharge variation (Cserkész-Nagy et al. 2010). Therefore, the Himalayan foothill rivers are generally dynamic and riverbank erosion–deposition is strongly related to the formation and shifting of meander bends. Channel migrations of alluvial rivers are the most common geomorphological features all over the earth's surface. Channel migration is the movement of the river channel within the valley over the historical time period (Kesel 2003). An alluvial channel migration in terms of time and space is controlled by both natural and anthropogenic factors (Rhoads et al. 2016). These controlling factors have shaped the physical form of the channel morphology (Chakraborty and Mukhopadhyay 2014). Due to decreased river gradient and discharge, lateral erosion becomes the most significant cause behind river migration (Ahmed et al. 2018). The river channel is subject to be eroded and deposited to reach the state of equilibrium (Xia et al. 2014). The mapping of changed channel position is significant for archiving the erosion hazards and changes in LULC, as well as for finding the causes of those changes (Debnath et al. 2017). Anthropogenic activities such as the construction of dams, channel straightening, removal of riparian vegetation, bridges across the rivers, alteration of bank materials, sand-gravel mining, intruding land

use, etc. are the most influential factors that lead to river channel migration. (Rhoads et al. 2016). Besides channel morphology is controlled by sediment load, channel resistance, nature of bedrock, discharge variability, embankment stability, floods, the slope of the river bed, and vegetation (Dhari et al. 2014).

For measuring, mapping, representing, and monitoring the morphodynamic features, effective tools, and techniques are very important. At present, remote sensing (RS) and geographical information systems (GIS) have enormous importance for change detection and mapping in rivers and their buffer zone dynamics at a different strategic scale (Wang and Mei 2016; Wang and Xu 2018). RS and GIS tools and techniques with field verification can accurately and quickly map and investigate river morphological changes (Rinaldi et al. 2013; Langat et al. 2018). In GIS-based spatial analysis, attributes both linear (here river bank) and areal (here floodplain area) segments of the study area have been considered for assessing the temporal trends. Therefore, the digital shoreline analysis system (DSAS) is a highly acceptable method, developed by the United States Geological Survey (USGS), capable to accurately measure the rate and predication of different river bankline positions (right and left bank separately) (Thieler et al. 2009; Ashraf and Shakir 2018; Jana 2019). Generally, the DSAS model has been used in the context of the sea shoreline. However, in the study of the river, the right and the left bank can be separately mapped with a higher degree of accuracy.

The area under study being situated in the seismo-tectonically unstable foothill terrain (Bhutan Himalaya) has produced an array of magnificent landscapes both physical and cultural involving multiple cycles of fluvial migration. The Raidak-I River is very important in terms of ecological variation. However, the previous literature indicates a relative vacuum of work in the geomorphological domain. This research is unique in terms of dynamic river studies in the geological and geomorphologically active or highly vulnerable areas of the Himalayan foothills of West Bengal. Especially, the effort to measure channel migration, erosion–deposition, and meander geometry parameters of the Raidak-I River buffer area is almost absent at the national level or local level. Therefore, this work attempts to measure the channel migration and erosion–deposition in the last 48 years timeframe. This work has been developed for estimating the historical bankline. Moreover, calculating channel migration, erosion–deposition, channel width, and channel sinuosity, is attempted using geospatial techniques coupled with field verification. Thus, the work intends to address the following objectives to study the morphodynamic changes of the Raidak-I River.

(i)   To estimate the nature of bankline oscillation using the DSAS method, and
(ii) To relate the channel oscillation with geomorphological and neotectonic controls.

2 Study Area

2.1 Location

A total of 81.9 km river stretch of Raidak-I River is selected for the present study which is the leftmost branch of the Raidak River that originates from the Himalayas and eventually meets Brahmaputra River in Bangladesh (Fig. 1). Spatially, River Raidak-I falls under two districts of West Bengal namely Cooch Behar and New Alipurduar. The latitudinal and longitudinal extent of the river is 26° 34′ 30.18″ N to 26° 12′ 57.58″ N and 89° 43′ 12.12″ E to 89° 41′ 38″ E. The Raidak River is amongst the main right bank tributaries of the Brahmaputra River. It is a trans-boundary river and flows through countries like Bhutan, India, and Bangladesh (Hasanuz-zanan and Mandal 2020). River Raidak has three courses: (1) the middle one is old Raidak, (2) western flow is named Raidak-I or Dipa-Raidak, and (3) the eastern one is named as Raidak-II. The studied river Raidak-I or Dipa-Raidak flows through Alipurduar District and enters in Tufanganj Subdivision in Cooch Behar District. Then it passes through the entire C.D. Block TufanganjI. During the path in Tufanganj Subdivision, the river is flowing through Balabhut, Bansraja, Debogram, Dhalpal,
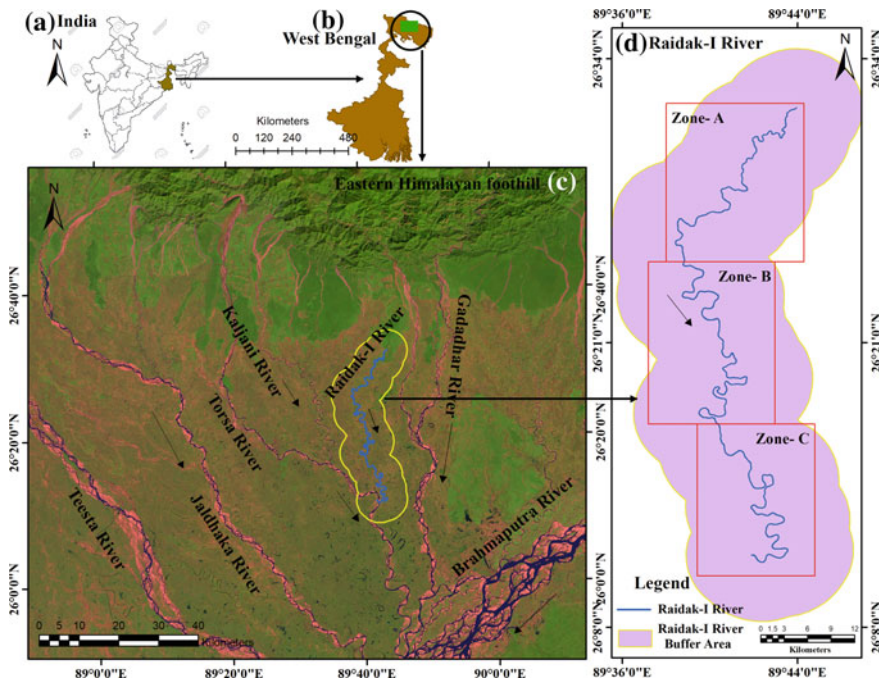
Fig. 1 Location map of the study area. **a** India. **b** West Bengal. **c** Eastern Himalayan foothill with study area. **d** Raidak-I River buffer area

Rajarkuthi, Shalbari, Dwiparpar, Andaranfulbari, Nakkatigachh, Kamatfulbari, and Chamta villages of the C.D. Block Tufanganj I. and enters Bangladesh to meet the Brahmaputra River.

2.2 Geology

The study area is a part of the extra-peninsula region, built up of rocks of ages ranging from Precambrian to Quaternary in various sections of the Himalaya Mountain and Ganga-Brahmaputra plain in eastern Himalaya (Banerji and Banerji 1979). The Quaternary deposits of the study area occur just south of the Siwalik group of formation and are constituted of boulders, gravels, pebbles, sands, and silts in the higher reaches forming alluvial fans and fluvial depositional terraces while mainly sands, silts, and clays in the lower reaches forming fluvial terraces of flood plain facies. Aggregates of boulders, pebbles and finer elastics exit on the levelled hilltops of BuxaDuar (Chattopadhyay and Das 1991). The rivers in this area are controlled by tectonism that gave rise to thrusting and normal faulting. The rivers change their slopes to adjust to geomorphic changes caused by the thrusts (Goswami et al. 2012). The study area is tectonically very active as it has experienced few earthquake events. According to Alam and Dominey-Howes (2016), seventeen above high to medium magnitude earthquake events were recorded during 1601–1984 in this region.

3 Materials and Methodology

3.1 Database

In this study, MSS, TM, ETM+ , and OLI datasets collected for 1972, 1979, 1987, 1995, 2003, 2011 and 2020 were used to demarcate the channel banklines (Table 1). All the satellite images were projected in the Universal Transverse Mercator (UTM) projection with zone 45 north and world geodetic survey 1984 (WGS84) datum and resampled in the ArcGIS environment. To maintain the data quality, all the images have been co-registered using the first-order polynomial model with the accuracy of root mean square error (RMSE) of less than 0.5 pixels with a minimum number (here it is 5) of ground control points (GCPs). Afterward, around 741 transects (on the left banks) and 922 (on the right bank) are generated for the estimation of riverbank shifting/erosion-accretion rate. Copernicus aerial imagery has also been used for river bank primary data verification.

Table 1 Characteristics of selected satellite images

Satellite images	Acquisition date	Path/row	Spatial resolution (in m)	Source
Landsat-1 MSS	21.12.1972	129/043	60	http://earthexplorer.usgs.gov
Landsat-1 MSS	16.12.1979	129/043	60	
Landsat-5 TM	08.12.1987	129/043	30	
Landsat-5 TM	19.12.1995	129/043	30	
Landsat-7 ETM+	16.01.2003	129/043	30	
Landsat-7 ETM+	05.01.2003	129/043	30	
Landsat-8 OLI-TIRS	27.12.2020	129/043	30	
ASTER DEM	2011		30	

3.2 Banklines Extraction

This process has been adopted for the assessment of earlier bankline positions with the help of selected satellite images. The bankline extraction is the process of transformation of the image, into a vector layer from raster data structure to determine right and left banklines separately on particular imagery (Jana 2019). We have used the normalized difference water index (NDWI) after McFeeters (1996), Haque et al. (2020) and modified normalized difference water index (MNDWI) (Xu 2006) for bankline extraction based on Eqs. (1) and (2) which employed green and NIR bands for segregation of land from water. Where pixels for water features are assigned as '1' and for land as '0' to achieve a binary image.

$$NDWI = Green - NIR/Green + NIR \tag{1}$$

To estimate the MNDWI, the MIR band of Landsat 7 and SWIR band of Landsat 5 and 8 along with the green band are also used. The technique for calculating the MNDWI was given by Xu (2006) as follows.

$$MNDWI = Green - MIR/Green + MIR \tag{2}$$

$$MNDWI = Green - SWIR/Green - SWIR \tag{3}$$

The output of these two ratios (NDWI and MNDWI) were further multiplied to generate another new image where the isolated pixel of the product image was nullified through the filtering technique of local mean matching (de Bethune et al. 1998) for detection of bankline position.

3.3 Estimation of Erosion–Deposition Rate

In the present work, the Digital Shoreline Analysis System (DSAS) extension tool of ArcGIS was used to assess the rate of bankline erosion-accretion by using the reference extracted baselines and auto-generated transects (Mandal et al. 2021). For the DSAS based statistical output, one further model has been employed such as the End Point Rate (EPR) model for computing present bankline erosion-accretion or shifting rate.

3.3.1 EPR Model for Calculating the Bankline Erosion-Accretion Rate

In the EPR model, based on the availability of data the considering period is divided into four temporal datasets i.e., 1973–1987, 1987–1997, 1997–2007, and 2007–2020. For each dataset, superimposed bankline positions have been portrayed and achieved a final line of overlapping visualization and this line is traced out as a composite line. Afterward, a buffer of 5 km distance from the composite line is drawn towards the right for the right bank and left for the left bank to demarcate the baselines. Therefore, several transects have been placed at a 50-m gap on the baseline which is created at the acute angle to the baseline up to 15 km distance away from both banks, and transects are auto-generated with ± 0.5 m uncertainties depending on the orientation of the baselines. Moreover, around 1347 transects (on the left banks) and 1456 (on the right bank) are placed along the baseline with 50 m spacing to cover the entire selected tract of the Raidak-I River (about 84.7 km) (Fig. 2).

$$EPR = \frac{Distance\ of\ bankline\ movement}{Time\ between\ oldest\ and\ most\ recent} \qquad (4)$$

In the EPR model, previous and recent data of two banklines are needed for this calculation and do not require any earlier knowledge regarding hydraulic interference or sediment transport. Moreover, this model is applied for two years of a data set viz. 1973–1987, 1987–1997, 1997–2007, and 2007–2020 for calculating the riverbank erosion-accretion rate which depicts the shifting trend over time.

The result of EPR is applied to calculate the rate of bankline migration and to understand the erosion-accretion nature (Mukhopadhyay et al. 2012; Jana 2019) using the 'Y' for positions of earlier (Y_{ob}) and recent (Y_{rb}) bankline. In this attempt, it is used as 'Y' to denote the projected bankline position which is estimated by Eq. (5).

$$Y = \alpha_{EPR} + \beta_{EPR}X \qquad (5)$$

where, X is the time interval ($X_{ob} - X_{rb}$) between earlier bankline (X_{ob}) and recent bankline (X_{rb}), α_{EPR} is model intercept, β_{EPR} denotes the rate of riverbank shifting (slope or regression coefficient).
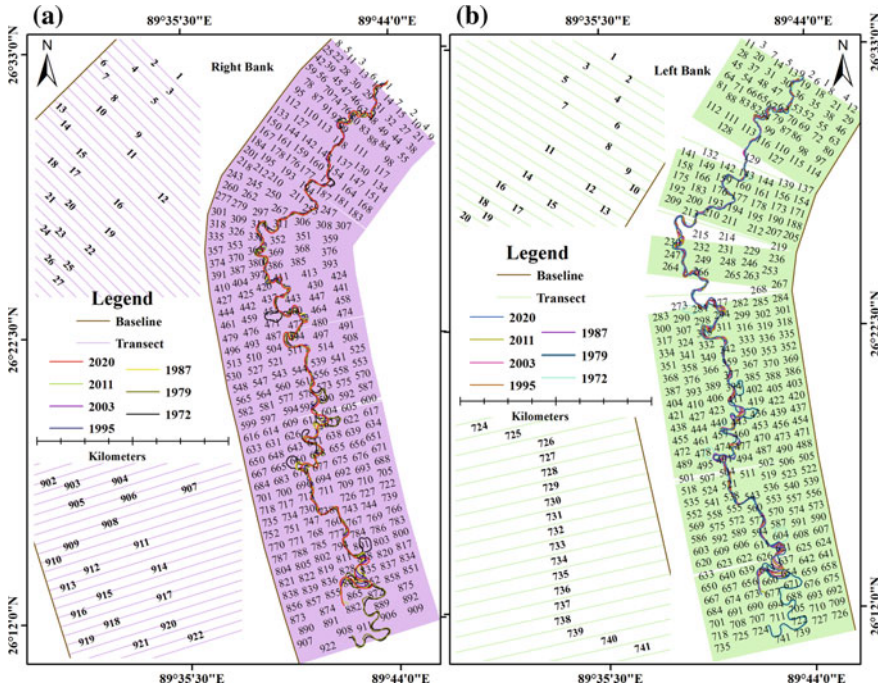
Fig. 2 Different banklines (1972–2020) are positioned along the baseline. All transects are oriented at angle with the corresponding baselines

On the other hand, the EPR intercept is calculated by Eq. (6).

$$\alpha_{EPR} = Y_{ob} - \left\{ \frac{Y_{ob} - Y_{rb}}{X_{rb} - X_{ob}} \right\} X_{ob} = Y_{rb} - \left\{ \frac{Y_{ob} - Y_{rb}}{X_{rb} - X_{ob}} \right\} X_{rb} \tag{6}$$

The rate of bankline migration for a given set of transects, the β_{EPR} is calculated by Eq. (7).

$$\beta_{EPR} = \left\{ \frac{Y_{ob} - Y_{rb}}{X_{rb} - X_{ob}} \right\} \tag{7}$$

3.4 Uncertainties and Errors

Potential errors are associated with satellite image-derived maps including datum changes, different surveying standards, projection errors, and distortions from uneven shrinkage, etc. (Anders and Byrnes 1991; Moore 2000). In the present study, four

different errors are identified for measuring the rate change and it may be of both positional and calculation-related errors. Calculation uncertainties are related to the skill and approach such as pixel error E_p, digitizing error E_d, and rectification error E_r and positional uncertainties are related to the features and phenomena that reduce the precision and accuracy of defining a bankline (both) position from a given data set such as; seasonal error E_s (Kankara et al. 2015). Finally, the total uncertainty value was estimated for each banklines by accounting for both positional and measurement uncertainties as follows.

$$E_t =_-^+ \sqrt{E_P + E_d + E_r + E_s} \qquad (8)$$

The weighted linear regression rate (WLR) is 2.4 m/yr for transect number 1347 (on the left bank) and 1456 (on the right bank) and the 87 percent confidence interval is 0.79 (Fig. 2). The band of confidence around the reported rate of change is -2.6 ± 0.78. In other words, it can be 87% confident that the true rate of change is between 3.25 and 1.78 m/yr. Also, R^2 (0.813) value justifies the acceptance of the work.

4 Channel Oscillation, Hydro-Geomorphic Drivers, and Active Tectonism

4.1 Channel oscillation

The riverbank shifting trend is estimated (Figs. 3 and 4) by considering the entire 48 years of data (1972–2020). As stated, the studied river stretch was segmented into the three distinct zones (A, B, and C) by spacing about 27 km based on the magnitude of meander geometry and the axial length of the river stretch in the middle-lower course. Moreover, around 247 transects (on the left banks) and 307 transects (on the right bank) are generated in the zone of A and B for estimation of riverbank shifting. However, in zone C, the number of transects is varied for different temporal spans due to spatio-temporal inconsistency of dynamic in the mouth of the river estuary. The temporal variation of river erosion–deposition for the year 1972–1979, 1979–1987, 1987–1995, 1995–2003, 2003–2011, and 2011–2020 are depicted in Fig. 8, that illustrates channel shifting of the Raidak-I River.

The result from 1972 to 1979 depicts that the average rate of bankline shifting in zone 'A' was -2.06 m/y at the left bank and 4.44 m/y at the right bank respectively. In zone 'B', the average rate of bankline shifting was -6.66 m/y (left bank) and 11.54 m/y (right bank). The rates of average bankline shifting in zone 'C' was 12.76 m/y and 14.47 m/y for the left and right bank, respectively. In this period, the overall average shifting of the left and right bank was 1.09 m/y and 10.04 m/y, respectively. The erosion–deposition rate and number of affected transects indicate that channel narrowing is caused by sediment accretion on bed areas of both the banks. Therefore, the dynamicity of the river was very high, especially in zone 'B' compared to other
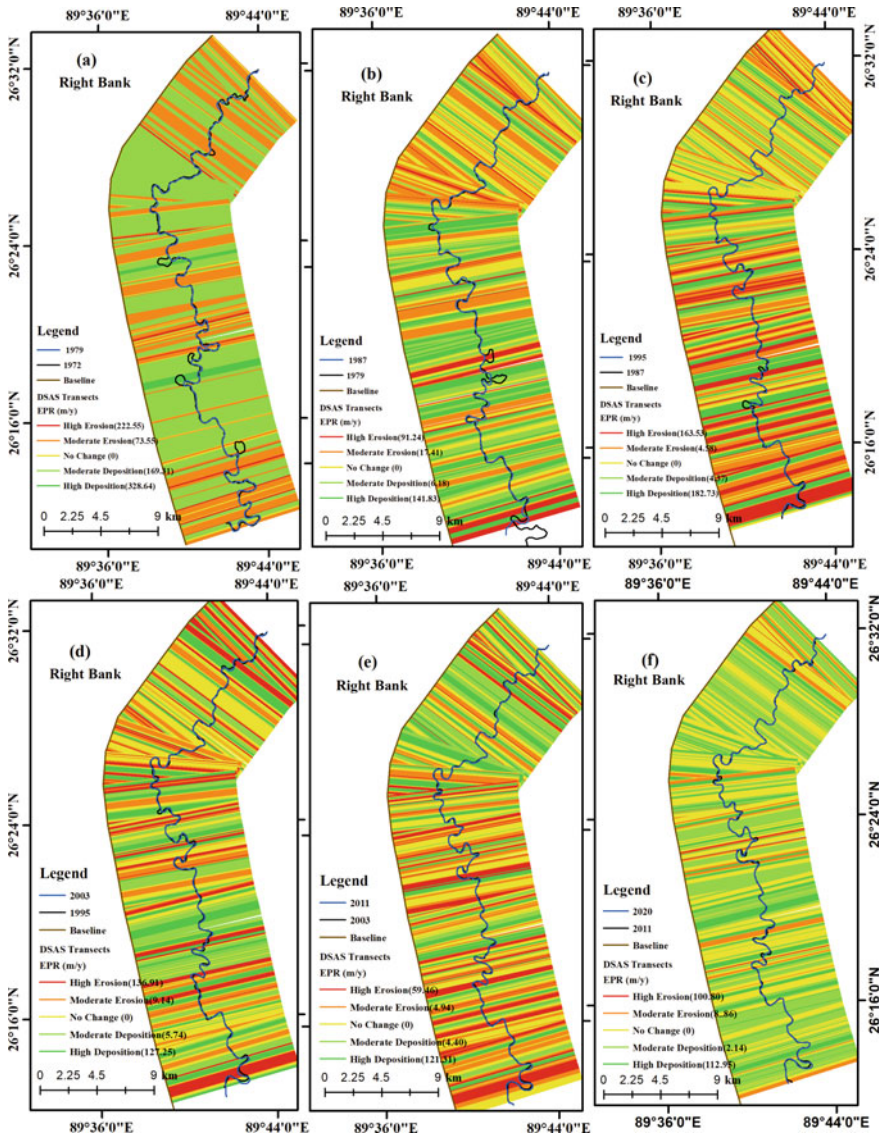
Fig. 3 Distribution of DSAS model derived riverbank erosion and deposition rate along transects during the different study periods, **a** 1972–1979, **b** 1979–1987, **c** 1987–1995, **d** 1995–2003, **e** 2003–2011, and **f** 2011–2020 at the right bank and **g** 1972–1979, **h** 1979–1987, **i** 1987–1995, **j** 1995–2003, **k** 2003–2011, and **l** 2011–2020 at the left bank
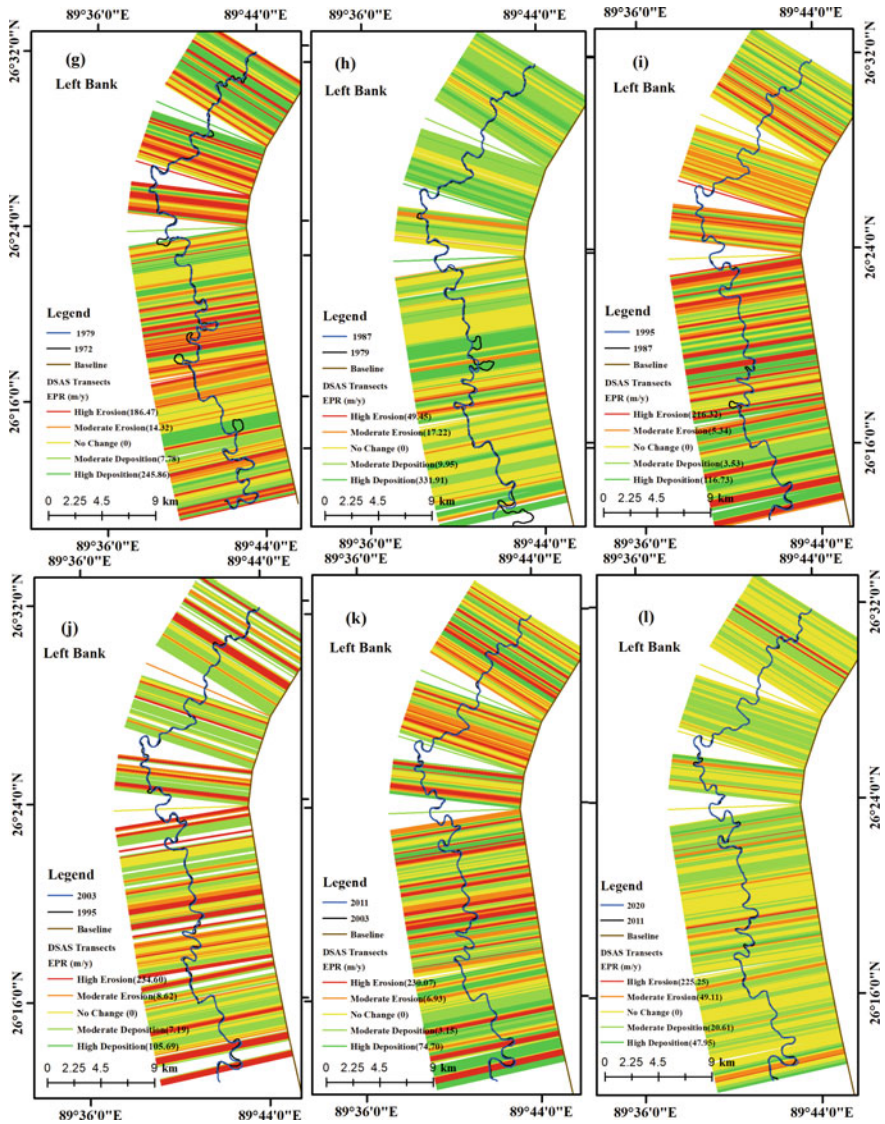
Fig. 3 (continued)

zones. From 1979 to 1987, zone 'A' was observed a higher rate of erosion–deposition on both banks (3.42 m/y at left bank and −5.20 at the right bank). On the other hand, in zone 'B' high deposition (10.35 m/y) was recorded in the left bank and also the high erosion (−2.24 m/y) in the right bank. Zone 'C' shows a rightward shifting of the river course with an average shifting rate of −5.54 m/y at the right bank and 8.26 m/y at the left bank. In general, during the period 1979 to 1987, the overall
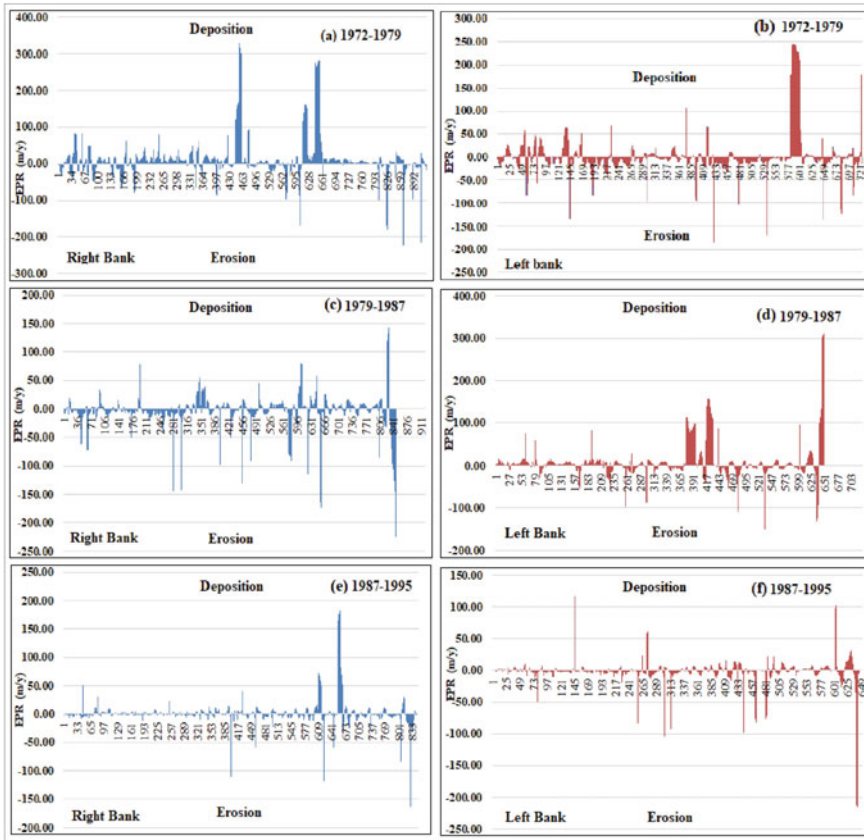
Fig. 4 DSAS model derived riverbank accretion-erosion during the periods of **a** 1972–1979, **c** 1979–1987, **e** 1987–1995, **g** 1995–2003, **i** 2003–2011, and **k** 2011–2020 at the right bank and **b** 1972–1979, **d** 1979–1987, **f** 1987–1995, **h** 1995–2003, **j** 2003–2011, and **l** 2011–2020 at the left bank

outward shifting rate was 7.22 m/y at the left bank and −4.12 m/y inward at the right bank, which indicates the rightward shifting of the river channel with its shrinking nature. As a result, the river channel migrates towards the right bank with a large extent of sedimentation at the left bank.

During 1987–1995, the average shifting rate in zone 'A' was −0.72 m/y for the left bank and 0.62 m/y for the right bank. In zone 'B', the rate of average shifting was −2.80 m/y for the left bank and 1.35 m/y for the right bank. Zone 'C' resulted in an average rate of channel migration with −1.71 and 0.75 m/y for the left and right bank, respectively. In this time frame, the average channel migration rate was −1.76 m/y (left bank) and 0.92 m/y (right bank), respectively. In this analysis, the left bank experienced extensive erosion. In this time period, the river has changed shifting direction from the right bank to the left bank. From 1995 to 2003, zone 'A'
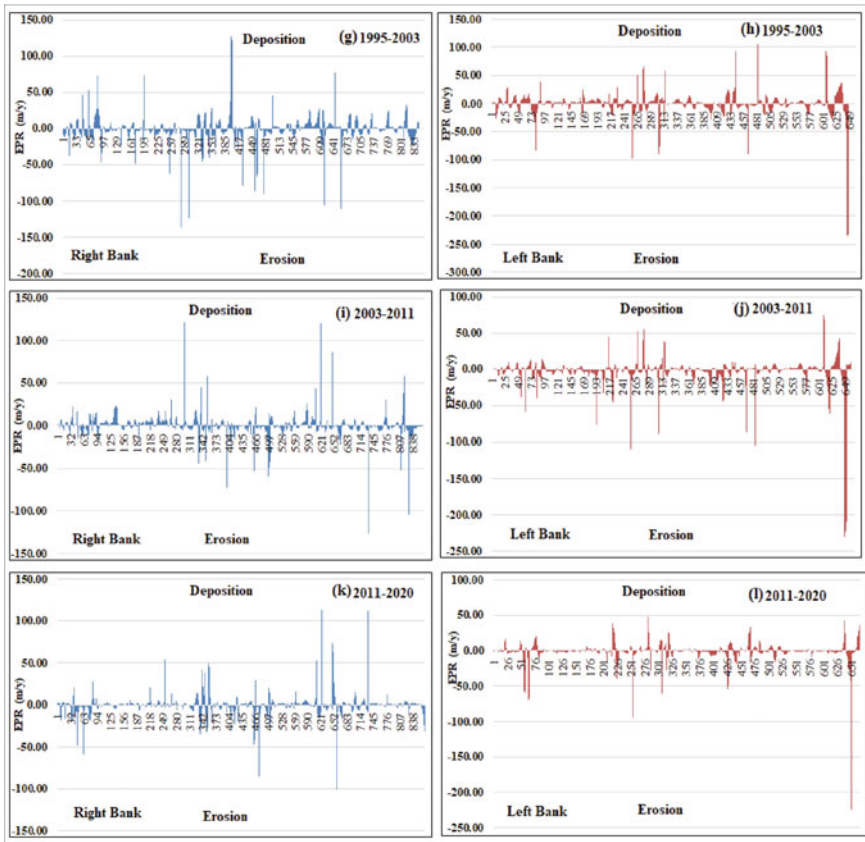
Fig. 4 (continued)

shows a high shifting rate (0.56 m/y) on the left bank and a high erosion rate on the right bank at −2.96 m/y. However, zone 'B' comprises significant erosion on both the left bank (−0.59 m/y) and the right bank (−0.42 m/y). Zone 'C' also passes through a relatively higher rate of erosion and it was estimated at −3.10 and −0.68 m/y on the left and right bank, respectively. In this time frame, the average channel migration rate was −0.73 m/y (left bank) and −1.32 m/y (right bank), respectively. The result from 2003 to 2011 depicts that the average rate of bankline shifting in zone 'A' was −3.04 m/y at the left bank and 2.40 m/y at the right bank respectively. In zone 'B', the average rate of bankline shifting was −3.55 m/y (left bank) and −1.05 m /y (right bank). The rates of average bankline shifting in zone 'C' were −3.52 and −1.86 m/y for the left and right bank, respectively. In this period, the overall average shifting of the left and right bank was −3.35 m/y and −0.05 m/y, respectively. In this observation, both bank experienced extensive erosion. During 2011–2020, the average shifting rate in zone 'A' is −0.79 m/y for the left bank and −1.09 m/y for the right bank. In zone 'B', the rate of average shifting is −

0.57 m/y for the left bank and −1.05 m/y for the right bank. Zone 'C' resulted in an average rate of channel migration with a figure of −1.60 and 0.14 m/y for the left and right bank, respectively (Fig. 4). In this time frame, the average channel migration rate is −0.92 m/y (left bank) and −0.65 m/y (right bank), respectively. The correspondence of high erosion at both banks is indicating channel widening. In this period (2003–2020), the overall negative (erosion) trend was observed for both banklines. This result indicates a widening river course triggered by persistent erosion on both banks. A general observation emanating from the present research is that the most dynamic or migrant part of the river is zone A and zone B compared to zone C which is relatively stable. In zone A, very active villages are Bakla, Chipra, Paschim, and PurbaKhalishamari for erosion and PurbaChikliguri, Uttar Parokata, and ChhotoChakirbas for deposition. In zone B, very active villages are Dhalpal, Chikliguri Dwitiakhanda, Guriarpur, and Basaraja Dwitia Khanda for erosion and Sikdarerkhata and Haripur for deposition. Kamat Phulbari, Balabhut, Dwiparpar, Debgram, Rajarkuthi, and Boalimohan Dwitia Khanda of zone C are very active for erosion-accretion and channel migration. In the timeframe of the last 48 years, the Raidak-I River has an average erosion–deposition at −0.23 m/year in the right bank and 1.57 m/y in the left bank. However, periodical migration values are regular and very considerable in terms of shifting. This investigation of the historical datasets has depicted the clear picture that the previous day deposition activity and present-day erosion activity are dominated. The Raidak-I River course has a high dynamic adjustment for their need and this changed channel behavior is very dramatic.

### 4.2 Hydro-Geomorphic Drivers and Active Tectonism

The riverbank erosion in the Himalayan foothill river course is triggered by a high gradient, high discharge of water and sediment load, meander geometry, bank material composition, and human interferences. However, the most crucial driving factors in the Raidak-I River are involved in fluid flow, which creates a significant impact on the flow regime of the river during the monsoon flood. Almost the entire amount of average annual rainfall (about 3444.04 mm) within the basin is received during the monsoon (June to September) (District Disaster Management Report 2009, Government of West Bengal, India). Thus, the bank margin allows rightward shifting the course and formed a dry gap with shrubs and grasses at the place of the former active channel. Also, near Dhalpal (zone B), the right bank has shifted about 224 m on the landward side (rightward) and 1 km distance along the bank through eroding agricultural land and embankment breaching. Such a condition is demonstrated by the EPR model-based riverbank shifting.

The geomorphological and tectonic adjustment in terms of channel migration and erosion–deposition can be undoubtedly depicted in terms of the changes of the river buffer zone that took place over space and time (Wallick et al. 2007; Bolton and Shellberg 2001). The Raidak-I River is bearing the imprint of active tectonics of the region as they lie in the zone of Himalayan Frontal Fault, the most active thrust belt

of the Himalayas (Das 2004; Goswami et al. 2012). Tectonic changes are depicted by the responses made in the adjoining morphology of this river behavior. Channel shifting and erosion–deposition may be modified directly or indirectly by an increase or decrease in slope imposed by areal uplift or subsidence. Sufficiently decreased slopes may cause rivers to transform along the path of meandering to the braided channel. The most commonly observed of these adjustments is for a meandering channel to increase its sinuosity in response to the increased slope, or decrease its sinuosity as an adjustment to the decreased slope (Holbrook, and Schumm 1999). Among the various causes, one of the most important causes of this river dynamicity is tectonic activity. In our analysis, the total erosion is greater than the deposition which indicates that this river is still actively engaged in fluvial erosion.

The hypsometric curve represents the different stages of the evolution of erosional landform (Strahler 1952). The basin age can be estimated through the value of the hypsometric integral (HI). The value of HI close to 1indicates its youthfulness of topography with the active pace of erosion while HI close to 0 denotes the old stage with the negligible rate of erosion (Schumm 1956; Strahler 1952). We have calculated the hypsometric integral as 0.15 which indicates that the Raidak-I River basin now falls into mature to the old stage.

The basin relief and size variations are represented in the long profiles of the river and stream length gradient index (SL Index). The distances and elevations were divided by maximum basin relief and the total stream length respectively to define the long profile (Lee and Tsai 2009). Thus, the presence of breaks in the river long profile depicts that a strong structural effect is somehow present in the river course. The long profile represents that the maximum portion of the river basin is included in plainland (Fig. 5). The SL Index is considered as a significant tool to detect local uplift as well as the incipient local response to regional processes (Troiani and Della Seta 2008). The SL Index was recorded high at the upper part of the river (Fig. 5). In this case, the union of morphological and morphometric evidence allows us to distinguish a sector in the Raidak-I River basin affected by active tectonic deformation. The hypsometric
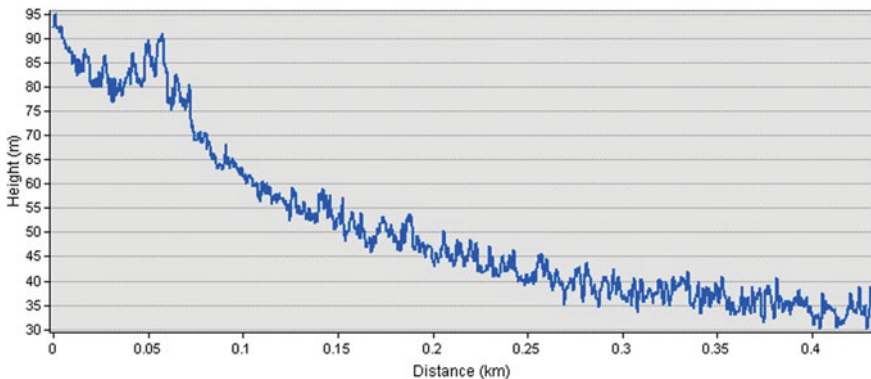

Fig. 5   a Long profile of the Raidak-I River Basin. **b** Stream Length Gradient Index (SL Index)

curve value, the SL Index, and the long profile properties provide adequate evidence of this river's low energy but the study result is different. This may be due to the energy boost-up that takes place in the river during extreme rainfall and floods. Moreover, the Bhutan Himalayas boulders, sand, and detritus are continuously deposited in these rivers causing the river beds to gradually rising (Saha and Bhattacharya 2019). This large sedimentation has choked the channel by the formation of countless islands and bars forcing the river to collapse the river banks and thus promoting continuous channel migration.

The hydrogeological map depicts that various formations of different ages and rock types have controlled the riverbank erosion–deposition activity of the Raidak-I River Basin (Fig. 6). The geological map depicts that Jalpaiguri and Shaugoan formations are the major control factors for the dynamicity of the river (Fig. 7). The geomorphological map of the study basin represents that piedmont and younger alluvial plain are dominant of the basin, which indicates that Raidak-I River is geomorphologically very unstable (Fig. 7). In our study, continuous channel adjustments have occurred in the Raidak-I River buffer area and the construction of various river regulation works along the river. In this analysis, both these processes such as natural (floods, geological activity), and anthropocentric activity (construction embankment and bridges) are playing an important role in geomorphological instability and various natural
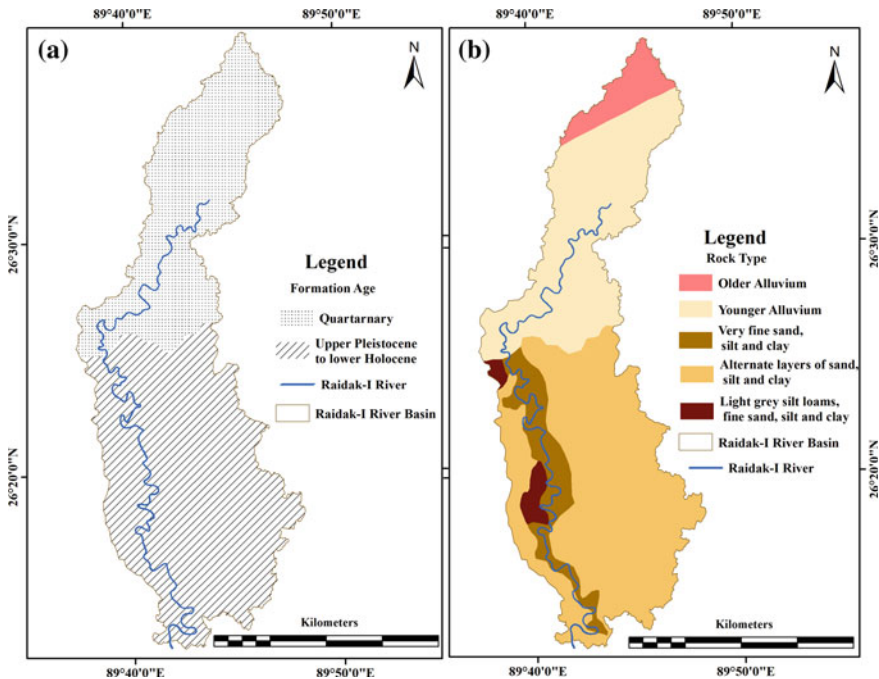
Fig. 6 Hydrogeological map of Raidak-I Basin. **a** Formation age, **b** Rock-type, *Source* Central Ground Water Board, India (CGWB and GIS)
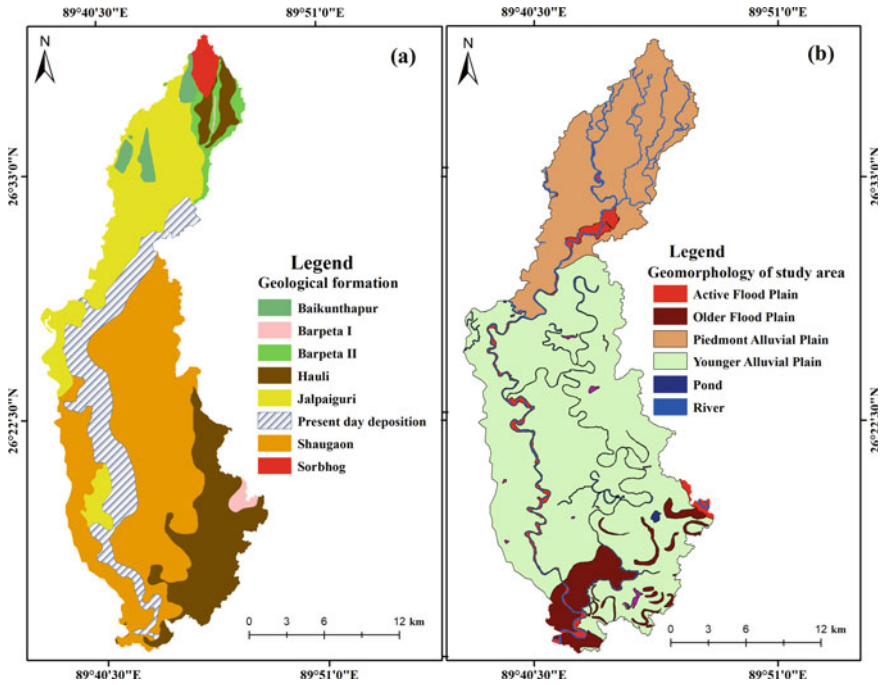
Fig. 7 Geomorphological and geological map of Raidak-I Basin. **a** Geological formation. **b** Geomorphology of the study area. *Source* Geological Survey of India

hazards. Therefore, this analysis has made a circumspect effort to provide insight into the historical channel migration and erosion–deposition of the study river in the sub-Himalayan piedmont region. It could help the administrators for understanding the relation between river migration and geomorphological adjustment.

4.3 Role of Embankment

The immense population pressure in the river corridor is exaggerated by controlling the natural channel flow pattern. The erosive meandering stretches are protected by strong embankment structures that are also able to divert the channel flow pattern. The diverted flow creates a harsh impact on the opposite bank through a severe rate of land erosion. Intensive sand mining activities also exaggerate the extensive riverbank erosion. Therefore, the riverbank shifts towards the left or right just after the embankment protected positions and adjusts its course with hydrodynamic behaviour. Thereafter, another new embankment is constructed at the recently exposed erosive section and robust controls the channel flow pattern which leads to channel narrowing. Also, at the positions of the bridge (across the river), the bridge protecting embankments
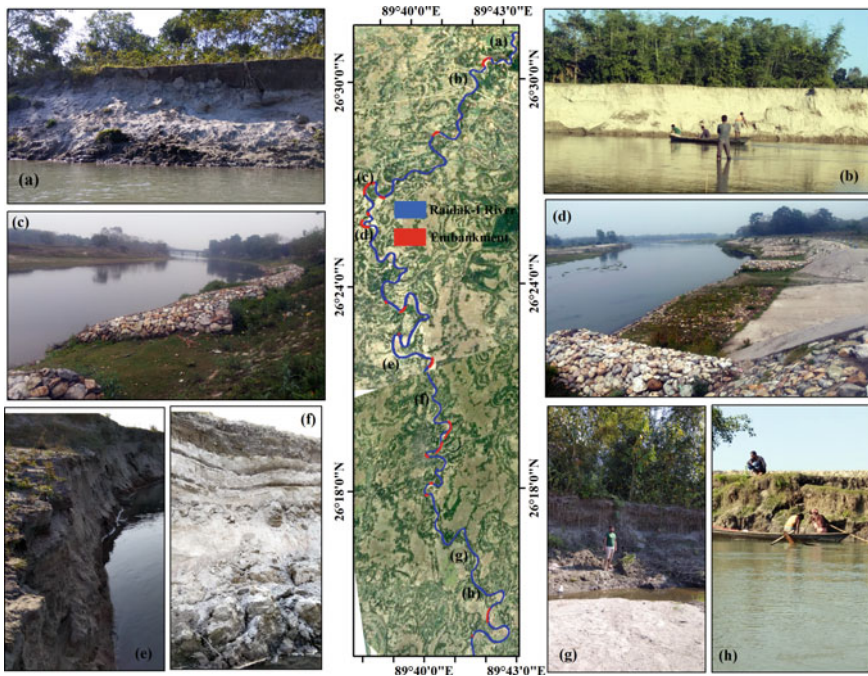
Fig. 8 Bridges and embankment along the Raidak-I River with field validation photos

are constructed along a concentrated part of the channel, is also insists on channel narrowing. The length of the river is 81.9 km in the present study, out of which 7.95 km long is attributed to embankments (Fig. 8). However, the channel hydraulic pattern has changed immediately after the bridge site by the widening of the channel. The overall result of erosion–deposition shows that to heavy extent erosion will take place in the inward position of the meander bend at the left bank and sediment deposition will occur in the straight course of the right bank. These will create a harsh impact on sediment feeding processes and resultant riverbank erosion/accretion in the course of the river. The riverbank erosion-accretion observation is a very important variable to planners, environmentalists, policymakers for understanding and formulating the needed and appropriate channel design schemes of vulnerable areas of the Raidak-I River.

5   Conclusion

This study has demonstrated the application and capability of earth observatory technology and generated a detailed evaluation of temporal and spatial changes in

river channel dynamics and adjustment of the Raidak-I River buffer area. The multi-temporal data analysis reveals that the Raidak-I River has continuously changed its bankline positions due to extensive erosion-accretion processes. In the timeframe of the last 48 years, the Raidak-I River has an average erosion–deposition at − 0.23 m/year in the right bank and 1.57 m/y in the left bank. A general observation from this whole research is that the most dynamic or migrant part of the river is zone A and zone B compared to zone C which is relatively stable. The study assesses the significant study regarding the dynamic change of river bankline positions in vulnerable areas and the endangered condition of the nearby settlements and infrastructures due to high bank erosion. Most hydrogeomorphological studies are focused on identifying factors causing the riverbank migration and erosion-accretion and its present situation. This work is a small effort to calculate the historical river bankline migration through an automated computational platform. Field validation and continuous monitoring are imperative for such types of automated approaches. Therefore, in the present research, the DSAS based automated approach is employed as an alternative way that successfully and accurately measures geomorphic processes (erosion-accretion) at an appropriate spatio-temporal scale. Moreover, it will be helpful for engineers, planners and administrators to take the appropriate management plans to save the river adjacent villages which are at the risk of severe bank erosion.

References

Ahmed I, Das N, Debnath J, Bhowmik M (2018) Erosion induced channel migration and its impact on dwellers in the lower Gumti River, Tripura, India. Spatial Information Research. https://doi.org/10.1007/s41324-018-0196-9

Alam E, Dominey-Howes D (2016) A catalogue of earthquakes between 810BC and 2012 for the Bay of Bengal. Nat Hazards 81(3):2031–2102. https://doi.org/10.1007/s11069-016-2174-7

Anders FJ, Byrnes MR (1991) Accuracy of shoreline change rates as determined from maps and aerial photographs. Shore Beach 59:17–26

Ashraf M, Shakir AS (2018) Prediction of river bank erosion and protection works in a reach of Chenab River, Pakistan. Arab J Geosci 11(7). https://doi.org/10.1007/s12517-018-3493-7

Banerji I, Banerji S (1979) A coalescing alluvial fan model of the Siwalik sedimentation a case study in the eastern Himalaya.Geol Surv India Miscellaneous Publ 41(1):1e12

Bastawesy M, White KH, Gabr S (2013) Hydrology and geomorphology of the Upper White Nile Lakes and their relevance for water resources management in the Nile basin. Hydrol Process 27:196–205. https://doi.org/10.1002/hyp.9216

Bolton S, Shellberg J (2001) Aquatic habitat guidelines white paper: ecological issues in floodplains and riparian corridors. Prepared for WA State Dept of Fish and Wildlife and others

Burbank DW, Anderson RS (2001) Tectonic geomorphology. Blackwell Publishing, 287 pp

Chakraborty S, Mukhopadhyay S (2014) An assessment on the nature of channel migration of River Diana of the sub-HimalayanWest Bengal using field and GIS techniques. Arab J Geosci. https://doi.org/10.1007/s12517-0141594-5

Chattopadhyay GS, Das A (1991) Quaternary geology and geomorphology of the Tista-Torsha interfluve area—a brief review. Geol Surv India Rec 118(pt 3–8):115–124

Cserkész-Nagy Á, Tóth T, Vajk Ö, Sztanó O (2010) Erosional scours and meander development in response to river engineering: middle Tisza region, Hungary. Proc Geol Assoc 121:238–247

Dai SB, Yang SL, Cai AM (2008) Impacts of dams on the sediment flux of the Pearl River, Southern China. Catena 76:36–43

Das JD (2004) Active tectonics of the Eastern Himalayan foothills region and adjoining Brahmaputra Basin based on satellite images. Int J Remote Sens 25(3):549–557. https://doi.org/10.1080/0143116031000148070

de Bethune S, Muller F, Donnay JP (1998) Fusion of multispectral and panchromatic images by local mean and variance matching filtering techniques. Fus Earth Data 28–30

Debnath J, Das (Pan) N, Ahmed I, Bhowmik M (2017) Channel migration and its impact on land use/land cover using RS and GIS: a study on Khowai River of Tripura, North-East India. Egypt J Remote Sens Space Sci 20(2):197–210. https://doi.org/10.1016/j.ejrs.2017.01.009

Dhari S, Arya DS, Murumkar AR (2014) Application of remote sensing and GIS in sinuosity and river shifting analysis of the Ganga River in Uttarakhand plains. Appl Geomat. https://doi.org/10.1007/s12518-014-0147-7

Goswami C, Mukhopadhyay D, Poddar BC (2012) Tectonic control on the drainage system in a piedmont region in tectonically active eastern Himalayas. Front Earth Sci 6(1):29–38. https://doi.org/10.1007/s11707-012-0297-z

Guchhait SK, Islam A, Ghosh S, Das BC, Maji NK (2016) Role of hydrological regime and flood-plain sediments in channel instability of the Bhagirathi River, Ganga-Brahmaputra Delta, India. Phys Geogr 37(6):476–510

Gurnell AM, Bertoldi W, Corenblit D (2012) Changing river channels: the roles of hydrological processes, plants and pioneer fluvial landforms in humid temperate, mixed load, gravel bed rivers. Earth Sci Rev 111(1–2):129–141. https://doi.org/10.1016/j.earscirev.2011.11.005

Haque SM, Kannaujiya S, Taloor AK, Keshri D, Bhunia RK, Champati Ray PK, Chauhan P (2020) Identification of groundwater resource zone in the active tectonic region of Himalaya through earth observatory techniques. Groundw Sustain Dev 10. Elsevier. https://doi.org/10.1016/j.gsd.2020.100337

Hasanuzzaman M, Mandal S (2020) A Morphology-independent Methodology to Assess Erosion, accretion and lateral migration of an alluvial channel using geospatial tools: a study on the Raidak-I River of Himalayan Foothills. Sustain Water Resourc Manag 6(3). https://doi.org/10.1007/s40899-020-00393-9

Holbrook J, Schumm SA (1999) Geomorphic and sedimentary response of rivers to tectonic deformation: a brief review and critique of a tool for recognizing subtle epeirogenic deformation in modern and ancient settings. Tectonophysics 305(1–3):287–306. https://doi.org/10.1016/s0040-1951(99)00011-6

Hooke JM (2013). River meandering, Treatise on geomorphology. Elsevier Ltd. https://doi.org/10.1016/B978-012-374739-6.00241-4

Islam A, Guchhait SK (2017a) Analysing the influence of Farakka Barrage Project on channel dynamics and meander geometry of Bhagirathi river of West Bengal, India. Arab J Geosci 10(11):1–18

Islam A, Guchhait SK (2017b) Search for social justice for the victims of erosion hazard along the banks of river Bhagirathi by hydraulic control: a case study of West Bengal, India. Environ dev sustain 19(2):433–459

Jana S (2019) An automated approach in estimation and prediction of riverbank shifting for flood-prone middle-lower course of the Subarnarekha River, India. Int J River Basin Manag 1–49. https://doi.org/10.1080/15715124.2019.1695259

Kankara RS, Selvan SC, Markose VJ, Rajan B, Arockiaraj S (2015) Estimation of long and short term shoreline changes along Andhra Pradesh coast using remote sensing and GIS techniques. Procedia Engineering 116:855–862. https://doi.org/10.1016/j.proeng.2015.08.374

Kesel RH (2003) Human modifications to the sediment regime of the Lower Mississippi River flood plain. Geomorphology 56:325–334

Kuehl SA, Allison MA, Goodbred SL, Kudrass H (2005) The Ganges-Brahmaputra Delta. Soc Sediment Geol 83:413–434

Kummu M, Lu XX, Rasphone A, Sarkkula J, Koponen J (2008) Riverbank changes along the Mekong River: remote sensing detection in the Vientiane–NongKhai area. Quatern Int 186(1):100–112

Langat PK, Kumar L, Koech R (2018) Understanding water and land use within Tana and Athi River Basins in Kenya: opportunities for improvement. Sustain Water Resourc Manag 1–11

Lee C, Tsai LL (2009) A quantitative analysis for geomorphic indices of longitudinal river profile: a case study of the Choushui River, Central Taiwan. Environ Earth Sci 1549–1558

Mandal BK, Islam A, Sarkar B, Rahman A (2021) Evaluating the spatio-temporal development of coastal aquaculture: an example from the coastal plains of West Bengal, India. Ocean Coast Manage 214:105922

McFeeters SK (1996) The use of the Normalized Difference Water Index (NDWI) in the delineation of open water features. Int J Remote Sens 17(7):1425–1432

Moore LJ (2000) Shoreline mapping techniques. J Coastal Res 16:111–124

Mukhopadhyay A, Mukherjee S, Mukherjee S, Ghosh S, Hazra S, Mitra D (2012) Automatic shoreline detection and future prediction: a case study on Puri Coast, Bay of Bengal, India. Eur J Remote Sens 45(1):201–213

Rhoads BL, Lewis QW, Andresen W (2016) Historical changes in channel network extent and channel planform in an intensively managed landscape: natural versus human-induced effects. Geomorphology 252:17–31. https://doi.org/10.1016/j.geomorph.2015.04.021

Rinaldi M, Surian N, Comiti F, Bussettini M (2013) A method for the assessment and analysis of the hydromorphological condition of Italian streams: the Morphological Quality Index (MQI). Geomorphology 180:96–108

Saha UD, Bhattacharya S (2019) Reconstructing the channel shifting pattern of the Torsa River on the Himalayan Foreland Basin over the last 250 years. Bulletin of geography. Physical geography series, no 16, pp 99–114 https://doi.org/10.2478/bgeo-2019-0007

Schumm SA (1956) Evolution of drainage systems and slopes in badlands at perthamboy, New Jersey. Geol Soc Am Bull 67(5):597. https://doi.org/10.1130/00167606(1956)67[597:eodsas]2.0.co;2

Starkel L, Sarkar S, Soja R, Prokop P (2008) Present-day evolution of the Sikkimese-Bhutanese Himalayan Piedmont, vol 219. Polska Akademia Naukinstytut Geografii I Przestrzennego Zagospodarowania, Prace Geograficzne, Warsaw, pp 62–70

Strahler AN (1952) Dynamic basis of geomorphology. Geol Soc Am Bull 63:923–938

Thieler ER, Himmelstoss EA, Zichichi JL, Ergul A (2009) Digital Shoreline Analysis System (DSAS) version 4.0—an ArcGIS extension for calculating shoreline change: U.S. Geological Survey Open-File Report 2008-1278

Troiani F, Della Seta M (2008) The use of the stream length–gradient index in morphotectonic analysis of small catchments: a case study from Central Italy. Geomorphology 102(1):159–168. https://doi.org/10.1016/j.geomorph.2007.06.020

Uddin K, Shrestha B, Alam MS (2011) Assessment of morphological changes and vulnerability of river bank erosion alongside the river Jamuna using remote sensing. J Earth Sci Eng 1:29–34

Wallick JR, Grant GE, Lancaster ST, Bolte JP, Denlinger RP (2007) Patterns and controls on historical channel change inthe Willamette River, Oregon, USA. In: Gupta A (ed) Largerivers: geomorphology and management. Wiley, pp 492–516

Wang S, Mei Y (2016) Lateral erosion/accretion area and shrinkage rate of the Linhe reach braided channel of the Yellow River between 1977 and 2014. J Geog Sci 26(11):1579–1592

Wang B, Xu YJ (2018) Dynamics of 30 large channel bars in the Lower Mississippi River in response to river engineering from 1985 to 2015. Geomorphology 300:31–44

Xia J, Zong Q, Deng S, Xu Q, Lu J (2014) Seasonal variations in composite riverbank stability in the lowerJingjiang reach China. J Hydrol 519:3664–3673

Xu H (2006) Modification of normalised difference water index (NDWI) to enhance open water features in remotely sensed imagery. Int J Remote Sens 27(14):3025–3033